

## Tip-enhanced Raman mapping with top-illumination AFM

This article has been downloaded from IOPscience. Please scroll down to see the full text article.

2011 Nanotechnology 22 175701

(<http://iopscience.iop.org/0957-4484/22/17/175701>)

View [the table of contents for this issue](#), or go to the [journal homepage](#) for more

Download details:

IP Address: 131.155.82.68

The article was downloaded on 18/03/2011 at 13:34

Please note that [terms and conditions apply](#).

# Tip-enhanced Raman mapping with top-illumination AFM

K L Andrew Chan and Sergei G Kazarian

Department of Chemical Engineering, Imperial College London, SW7 2AZ, UK

E-mail: [s.kazarian@imperial.ac.uk](mailto:s.kazarian@imperial.ac.uk)

Received 2 January 2011, in final form 10 February 2011

Published 16 March 2011

Online at [stacks.iop.org/Nano/22/175701](http://stacks.iop.org/Nano/22/175701)

## Abstract

Tip-enhanced Raman mapping is a powerful, emerging technique that offers rich chemical information and high spatial resolution. Currently, most of the successes in tip-enhanced Raman scattering (TERS) measurements are based on the inverted configuration where tips and laser are approaching the sample from opposite sides. This results in the limitation of measurement for transparent samples only. Several approaches have been developed to obtain tip-enhanced Raman mapping in reflection mode, many of which involve certain customisations of the system. We have demonstrated in this work that it is also possible to obtain TERS nano-images using an upright microscope (top-illumination) with a gold-coated Si atomic force microscope (AFM) cantilever without significant modification to the existing integrated AFM/Raman system. A TERS image of a single-walled carbon nanotube has been achieved with a spatial resolution of  $\sim 20\text{--}50$  nm, demonstrating the potential of this technique for studying non-transparent nanoscale materials.

(Some figures in this article are in colour only in the electronic version)

## 1. Introduction

Tip-enhanced Raman mapping is potentially a very powerful analytical technique. It combines the high spatial resolution offered by an atomic force microscope (AFM) with the high chemical specificity of Raman spectroscopy. A typical approach in a TERS experiment is to focus the laser beam at a metal tip with the light polarized along the tip axis and to collect the surface-enhanced Raman scattered light from the sample in the enhancement zone of the tip using corresponding optics. One of the first TERS experiments achieved this by adapting the inverted mode configuration which involves illuminating samples from below with a tip approaching from above [1]. While this arrangement has the advantage of high collection efficiency, it is limited to the study of transparent samples only. For opaque samples, the tip and laser beam will have to be introduced from one side or coated transparent probes will have to be used for illumination [2, 3]. Sun and Shen have shown that TERS images can be obtained in an upright microscope by adding a small mirror to direct the focusing laser light to the tip [4]. In this arrangement, the laser is, effectively, side-illuminating the tip and the angle of incidence can be adjusted in order to maximize the enhancement effect. Another approach also found to be

effective was using a side-illuminating objective to focus the laser light at the tip while collecting the scattered light either from the same objective [5] or from an upright objective [6]. This method has been applied to image carbon nanotube [7] molecules deposited on a gold surface [8] and to study the strain distribution on silicon wafers [4, 9, 10]. Apart from the side-illumination, a parabolic mirror with a numerical aperture (NA) of one has also been used to increase the efficiency of signal collection as well as to generate a desirable polarization for the maximum enhancement effect [11–13]. The advantages and disadvantages of top-illuminated and inverted geometries have been discussed in a recent publication [14]. Relatively few examples of tip-enhanced Raman mapping have been demonstrated using an upright microscope where laser beam and scattered light are focused and collected from the same upright microscope objective due to the difficulties in avoiding shadowing of the scattered signals from the AFM tip. Schultz *et al* [15] adapted a similar system employed by Sun and Shen [4] and obtained TERS image of carbon nanotubes without the added side mirror. In this work, a glass AFM tip with a  $<200$  nm gold nanoparticle at the tip end and a radially polarized laser beam were used. Since the nanoparticle was relatively large, the spatial resolution reported was of the order of 125 nm. Recently, Stadler *et al* [16] published a work on a

top-illuminated TERS experiment of a thin film of dyes on gold surfaces in gap mode (the thin sample is located between a gold surface and a silver tip) using a scanning tunneling microscopy (STM) approach. A spatial resolution of at least 15 nm and an enhancement level of  $\sim 10^7$  have been reported. Since the measurement is based on STM and gap mode, it is currently limited to studying very thin conductive samples. In this work, we demonstrate the possibility of obtaining TERS images with a high spatial resolution using a gold-coated Si AFM tip in top-illumination mode using an upright microscope with a linearly polarized laser beam. The measurement can be performed on any substrates and it is demonstrated without the use of gap mode.

## 2. Experimental details

TERS images were obtained using an integrated system which consists of an upright microscope with an 100 $\times$  long working distance objective (NA of 0.7) and an integrated AFM head (NTEGRA, NT-MDT), a Raman spectrometer (nVia Raman Microscope, Renishaw, UK) with a 633 nm HeNe laser and a 1024 pixels  $\times$  400 pixels CCD (Andor detector) connected to the microscope/AFM system (NTEGRA Spectra, NT-MDT). A schematic of the TERS system setup is shown in figure 1. The location of the laser spot can be precisely controlled by a mirror with a piezomotor such that the laser spot can be aligned to the AFM tip. The sample is placed on an XYZ piezo-stage. In this design, the laser beam is focused and the scattered light is collected by the same objective.

Contact mode Si AFM tips (ATEC-CONT, Nanosensors) were sputtered with a thin layer of gold coating (K550X, Emitech, Quorum Technologies, UK) under the condition of  $10^{-1}$  mbar of argon, a coating current of 35 mA, 45 mm distance from the sputtering source and 2 min of coating time. The soft piezo-approach technique was adapted to avoid damage of the gold on the tip and the lowest contact pressure settings were used to minimize the impact between the tip and sample [17]. The laser beam at a power of <1 mW was used. An aperture was inserted to mask the laser beam such that the backscattering of the laser light from the back of the cantilever was minimized. The laser was focused on the sample and the apex of the gold-coated AFM tip. This was achieved by scanning the laser beam, by moving the mirror, across the approaching tip. Whenever the laser spot entered the tip area, an apparent small increase in fluorescent background was noticed. The area with the strongest background is regarded as the 'hot spot'. The sample was scanned by moving the XYZ piezo-stage, and the topography image and the tip-enhanced Raman image were collected simultaneously. One second integration time was used to collect the Raman signal at each point of the image. Data analysis was performed using the Nova software (NT-MDT).

Carbon nanotubes (P2-SWNT, Carbon Solutions) were sonicated in solvent (chloroform) for 2 h followed by spreading on a glass substrate. The solvent was evaporated at room temperature under a fume hood. The sample was stored at room condition until being used.

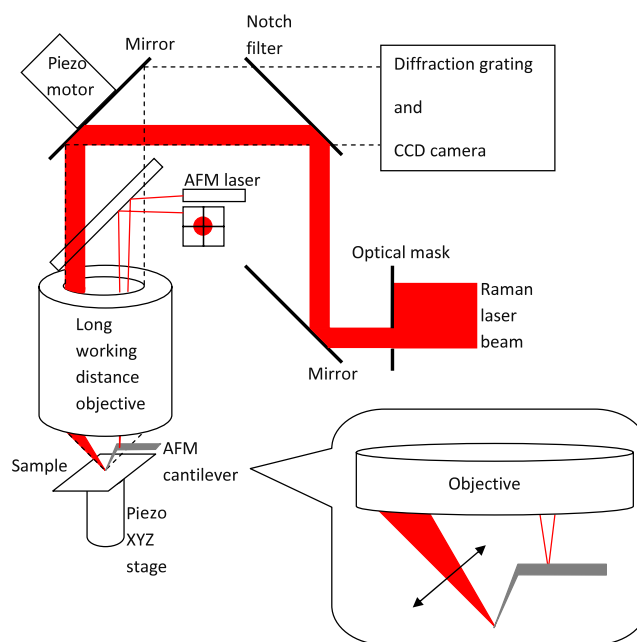


**Figure 1.** A schematic diagram showing the arrangement of the TERS system (NTEGRA Spectra) in an upright configuration. Note that the objective is used to focus laser light on the sample as well as to collect the scattered light at the spectrometer. The scattered light is shown with the dotted line boundaries.

## 3. Results and discussion

The Si tip employed in this study is called the 'tip at the end of the cantilever<sup>TM</sup>', where the tip protrudes out from the end of the cantilever such that shadowing from the cantilever is minimized. The tip contacts the sample at an angle of  $\sim 20^\circ$  from the normal to the surface of the sample (see inset in figure 1). To maximize the tip enhancement effect, the polarization of the laser light should be parallel to the tip axis [18]. In upright configuration, this can be achieved by using a radially polarized light [19, 20] and it has been applied in TERS studies [19, 21, 15]. However, when using side-illumination, this also can be achieved with the linear polarized light [22]. Here we employ a technique that will create a side-illumination with the unmodified upright objective allowing the experiment to be carried out with linear polarized laser light. This was achieved by masking  $\sim 4/5$  of the laser beam that enters the objective which eventually only illuminates the sample from the opposite to the cantilever side (the left-hand side, see figure 1). The angle of incidence of the laser beam was just below  $45^\circ$  based on the fact that the NA of the objective was 0.7. While the angle of incidence of the laser light did not align with the axis of the tip exactly, it was the closest match with the current setup. Since the AFM tip and the laser beam approach the sample from the same side and the cantilever employed in this study was not transparent, the back of the cantilever will be shadowing that part of the objective. The introduced mask, in this case, also has the advantage of reducing the scattered light from the top surface of the cantilever. While the  $\sim 4/5$  of the laser beam is masked, the scattered light collected by the same objective is only

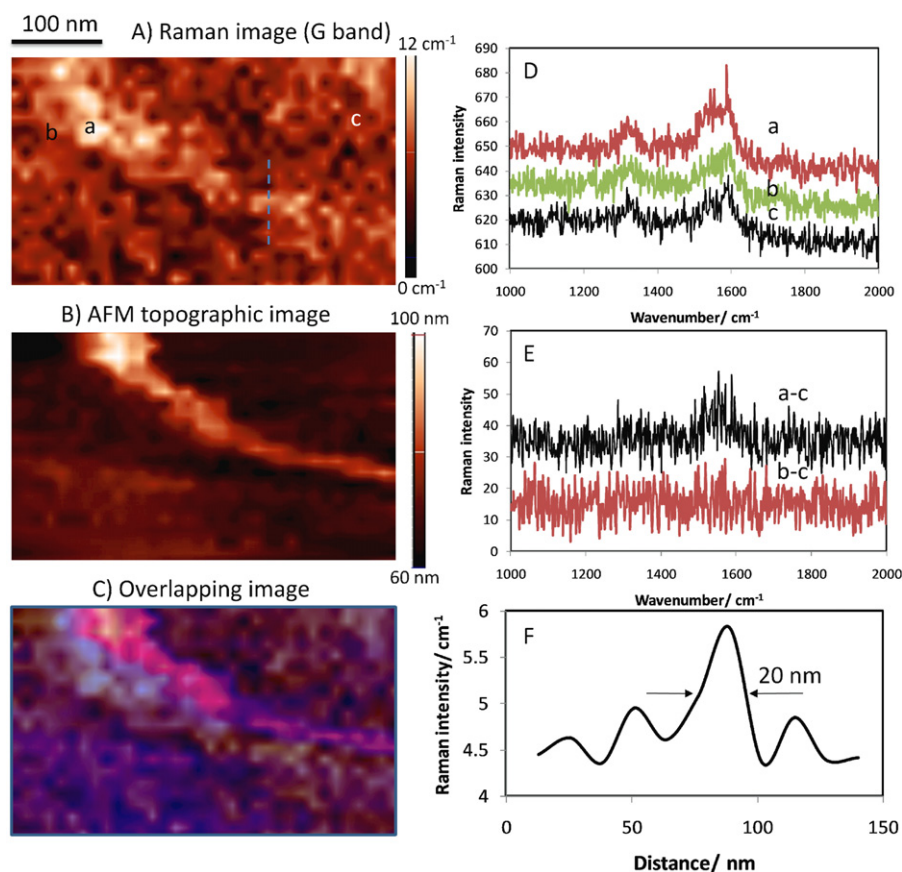


**Figure 2.** (A) TERS image of a carbon nanotube. The image is generated based on the changes in the area under the G band at  $\sim 1590\text{ cm}^{-1}$  across the mapped region with the baseline area subtracted. (B) AFM topographic image of the same area of sample measured simultaneously. (C) An overlapping image of (A) and (B). (D) Extracted spectra from locations indicated on image (A). (E) Difference spectra of a and c (the spectrum extracted from nanotube region a, subtracting the spectrum from non-nanotube region, c) and b and c (the spectrum extracted from  $\sim 50\text{ nm}$  away from nanotube region b, subtracting the spectrum extracted from non-nanotube region c). (F) The Raman intensity profile across the dotted line indicated on image (A).

shadowed by the cantilever which is blocking less than a half of the objective.

The AFM system can be operated in two possible modes: semi-contact mode or contact mode. In contact mode, the sample is always in contact with the gold-coated tip and it is exposed to the intense enhancement zone of the tip apex. On the other hand in semi-contact mode, the tip is oscillating such that the sample only enters the enhancement zone near the tip apex at a regular time interval. Previous studies [7, 23] have shown that the tip enhancement effect diminishes within 5–15 nm between a sample and a tip. To achieve the maximum enhancement in semi-contact mode, a setting that would give a small oscillation at an amplitude of 5–10 nm was adapted. However, in this study, it was not possible to obtain any TERS signal from the gold-coated tips when operating in semi-contact mode even when the amplitude of the oscillation was reduced to  $\sim 5\text{ nm}$ . Schultz *et al* [24] suggested that when the TERS experiment is carried out with linear or azimuthally polarized laser beams, the enhancement zone at the tip is along the  $X$  and  $Y$  directions rather than at the  $Z$  axis along the tip. Furthermore, the polarization of the laser light was not aligned exactly with the tip axis, hence, the enhancement effect is diminished even when the tip is just a few nanometers away from the surface. With the setup presented in this work, The

TERS effect was only observed when the system was operated in the contact mode. Note that when the tip is scanning very near the sample, as in most of the TERS experiments, the comparison of Raman signals between tip approaching and tip retracting does not always provide the certainty of having TERS signals. When the AFM is operated in contact or even in semi-contact mode the tip is in close proximity to the sample, so a small amount of material can be transferred to the tip, thus providing a false enhancement of Raman signal when the tip is approaching. It is therefore important to check if the apparent enhancement is sensitive to the location of the tip related to the sample. This is automatically achieved when an image is scanned. When an image is obtained by scanning the tip across the sample, only a TERS active tip provides a distribution map at a spatial resolution that is better than what can be achieved with a conventional confocal microscope. In all the images that were scanned in semi-contact mode, no improvement in spatial resolution was observed based on the carbon nanotube distribution map despite the apparent increase in carbon nanotube signals when comparing the Raman signals obtained with the tip approaching and tip retracting.

When the tip scans in contact mode, fine features of the individual carbon nanotubes can be observed and the result is shown in figure 2. The Raman image is generated based on the

G band of the carbon nanotube at  $\sim 1590\text{ cm}^{-1}$  (figure 2(A)) and is simultaneously obtained with the topographic image (figure 2(B)). The close agreement between the topographic image and the Raman image and the high spatial resolution obtained has ensured that a TERS image has been successfully obtained with this upright configuration. Spectra have been extracted from the locations marked on figure 2(A). The spectrum extracted from a location far away ( $>300\text{ nm}$ ) from the carbon nanotubes has shown a weak signal of the carbon nanotube (spectrum c in figure 2(D)) which is indicative of some small amounts of carbon nanotubes being transferred to the tip surface, which has emphasized the importance of the comparison of the Raman signal obtained from different locations of the sample to ensure that the enhanced signal is from the TERS effect rather than from the contamination of the tip. Comparison of that spectrum with the one extracted from an area near the carbon nanotube ( $\sim 50\text{ nm}$  away from the carbon nanotube) has shown that the contribution from far-field Raman signals was very small. The difference spectrum is shown in figure 2(E) which demonstrated that the far-field signal is not noticeable while the enhanced signal can be clearly seen. A Raman intensity profile across the carbon nanotube region has been extracted and is shown in figure 2(F). From this profile, the full width at half maximum was estimated to be  $\sim 20\text{--}50\text{ nm}$  (a range was indicated here because the noise level of the image prevents a more accurate estimation of the spatial resolution from this figure), which is similar to previous results reported by others with a side-illuminating objective [7].

When the topographic image is overlapped with the simultaneously obtained TERS images using the contact mode measurement (figure 2(C)), one can notice that the TERS image of the carbon nanotubes is slightly offset lower to the topographic image by approximately  $35\text{ nm}$ . This indicates that the enhancement zone is on the side of the tip apex rather than at the end of the tip. We suggest that this is caused by the mismatch between the angle of the tip and the angle of incidence of the laser light with the normal linear polarization, which also explains why it was difficult to observe any enhancement in semi-contact mode where the tip was not directly in contact with the sample most of the time. Taking the images in figure 2 as the reference, the cantilever is located on the top side of the image and the laser is illuminated from the bottom side, unlike what has been shown in figure 1 which indicates that the laser was illuminated from the left. (It has been shown in this way for a more clear illustration of how the tip was illuminated rather than showing the actual orientation of the laser and tip relative to the image orientation.) The observed offset can then be understood by considering the laser beam to be approaching the tip from the bottom side of the image. Interestingly the enhancement is observed only to one side of the nanotube rather than both sides, suggesting that the enhancement zone is only formed at one side of the tip. This actually results in a better spatial resolution than in the case where the enhancement zone surrounded all of the tip end. Nevertheless, there are opportunities to further improve the current setup to maximize the enhancement signals, for example by introducing a tilt to the tip or modifying that tip to

match the angle of incidence of the laser light or to use radially polarized light. Very recently, Raschke and co-workers [25] have demonstrated the possibility of obtaining TERS spectra from thick samples using adiabatic plasmon focusing into the tip apex region for better efficiency of TERS. Significantly improved TERS spectra have been reported but as yet without imaging data [25].

#### 4. Conclusions

In this work, we have demonstrated that TERS images with nanometer spatial resolution can be obtained by using an upright microscope and a gold-coated Si AFM cantilever working in contact mode with top-illumination. The approach involved introducing a mask to the laser light to create a side-illumination effect while collecting the scattered light with the same upright microscope objective. Shadowing from the cantilever was minimized by employing a 'tip at the end of the cantilever' type AFM probe. However, no TERS images can be obtained when the AFM is operating in semi-contact mode in this setup, suggesting that the enhancement zone was created at the side rather than at the bottom of the AFM tip. With the current setup, the polarization of the laser light was not perfectly aligned to the axis of the tip, leaving the opportunity for further improvement of the enhancement level that may be achieved in this upright mode. The spatial resolution achieved with this system in the upright rather than the inverted configuration was  $\sim 20\text{--}50\text{ nm}$ , demonstrating the potential of this technique to study non-transparent nanoscale materials without limitation on sample conductivity.

#### Acknowledgment

SGK acknowledges the research funding from the European Research Council under the European Community's Seventh Framework Programme (FP7/2007-2013)/ERC advanced grant agreement no. [227950].

#### References

- [1] Stockle R M, Suh Y D, Deckert V and Zenobi R 2000 Nanoscale chemical analysis by tip-enhanced Raman spectroscopy *Chem. Phys. Lett.* **318** 131–6
- [2] Jahncke C L, Paesler M A and Hallen H D 1995 Raman imaging with near-field scanning optical microscopy *Appl. Phys. Lett.* **67** 2483–5
- [3] Hallen H D, LaRosa A H and Jahncke C L 1995 Near-field scanning optical microscopy and spectroscopy for semiconductor characterization *Phys. Status Solidi a* **152** 257–68
- [4] Sun W X and Shen Z X 2003 Apertureless near-field scanning Raman microscopy using reflection scattering geometry *Ultramicroscopy* **94** 237–44
- [5] Saito Y, Motohashi M, Hayazawa N, Iyoki M and Kawata S 2006 Nanoscale characterization of strained silicon by tip-enhanced Raman spectroscopy in reflection mode *Appl. Phys. Lett.* **88** 143109
- [6] Mehtani D, Lee N, Hartschuh R D, Kisliuk A, Foster M D, Sokolov A P and Maguire J F 2005 Nano-Raman spectroscopy with side-illumination optics *J. Raman Spectrosc.* **36** 1068–75

- [7] Roy D, Wang J and Welland M E 2006 Nanoscale imaging of carbon nanotubes using tip enhanced Raman spectroscopy in reflection mode *Faraday Discuss.* **132** 215–25
- [8] Pettinger B, Ren B, Picardi G, Schuster R and Ertl G 2004 Nanoscale probing of adsorbed species by tip-enhanced Raman spectroscopy *Phys. Rev. Lett.* **92** 096101
- [9] Hartschuh R D, Lee N, Kisliuk A, Maguire J F, Green M, Foster M D and Sokolov A P 2007 *Frontiers of Characterization and Metrology for Nanoelectronics* ed D G Seiler *et al* (Melville: American Institute of Physics) pp 549–52
- [10] Saito Y, Motohashi M, Hayazawa N and Kawata S 2008 Stress imaging of semiconductor surface by tip-enhanced Raman spectroscopy *J. Microsc.* **229** 217–22
- [11] Stanciu C, Sackrow M and Meixner A J 2008 High NA particle- and tip-enhanced nanoscale Raman spectroscopy with a parabolic-mirror microscope *J. Microsc.* **229** 247–53
- [12] Sackrow M, Stanciu C, Lieb M A and Meixner A J 2008 Imaging nanometre-sized hot spots on smooth Au films with high-resolution tip-enhanced luminescence and Raman near-field optical microscopy *ChemPhysChem* **9** 316–20
- [13] Zhang D *et al* 2009 Parabolic mirror-assisted tip-enhanced spectroscopic imaging for non-transparent materials *J. Raman Spectrosc.* **40** 1371–6
- [14] Berweger S and Raschke M B 2010 Signal limitations in tip-enhanced Raman scattering: the challenge to become a routine analytical technique *Anal. Bioanal. Chem.* **396** 115–23
- [15] Schultz Z D, Stranick S J and Levin I W 2008 Tip-enhanced Raman spectroscopy and imaging: an apical illumination geometry *Appl. Spectrosc.* **62** 1173–9
- [16] Stadler J, Schmid T and Zenobi R 2010 Nanoscale chemical imaging using top-illumination tip-enhanced Raman spectroscopy *Nano Lett.* **10** 4514–20
- [17] Chan K L A and Kazarian S G 2010 Finding a needle in a chemical haystack: tip-enhanced Raman scattering for studying carbon nanotubes mixtures *Nanotechnology* **21** 445704
- [18] Novotny L and Stranick S J 2006 Near-field optical microscopy and spectroscopy with pointed probes *Annu. Rev. Phys. Chem.* **57** 303–31
- [19] Hayazawa N, Saito Y and Kawata S 2004 Detection and characterization of longitudinal field for tip-enhanced Raman spectroscopy *Appl. Phys. Lett.* **85** 6239–41
- [20] Quabis S, Dorn R and Leuchs G 2005 Generation of a radially polarized doughnut mode of high quality *Appl. Phys. B* **81** 597–600
- [21] Roy D and Williams C 2010 High resolution Raman imaging of single wall carbon nanotubes using electrochemically etched gold tips and a radially polarized annular beam *J. Vacuum Sci. Technol. A* **28** 472–5
- [22] Hayazawa N, Tarun A, Inouye Y and Kawata S 2002 Near-field enhanced Raman spectroscopy using side illumination optics *J. Appl. Phys.* **92** 6983–6
- [23] Pettinger B, Domke K F, Zhang D, Picardi G and Schuster R 2009 Tip-enhanced Raman scattering: influence of the tip-surface geometry on optical resonance and enhancement *Surf. Sci.* **603** 1335–41
- [24] Schultz Z D, Stranick S J and Levin I W 2009 Advantages and artifacts of higher order modes in nanoparticle-enhanced backscattering Raman imaging *Anal. Chem.* **81** 9657–63
- [25] Berweger S, Atkin J M, Olmon R L and Raschke M B 2010 Adiabatic tip-plasmon focusing for nano-Raman spectroscopy *J. Phys. Chem. Lett.* **1** 3427–32